Estuarine, Coastal and Shelf Science 244 (2020) 106101

Contents lists available at ScienceDirect

Estuarine, Coastal and Shelf Science

journal homepage: www.elsevier.com/locate/ecss

Groundwater dynamics in a restored tidal marsh are limited by historical soil compaction

Niels Van Putte[a,*], Stijn Temmerman[a], Goedele Verreydt[a,e], Piet Seuntjens[b,c], Tom Maris[a], Marjolein Heyndrickx[d], Matthieu Boone[d], Ingeborg Joris[b,f], Patrick Meire[a]

[a] University of Antwerp, Department of Biology, Ecosystem Management Research Group, Universiteitsplein 1C, 2610, Wilrijk, Belgium
[b] VITO - Flemish Institute for Technological Research NV, Unit Environmental Modeling, Boeretang 200, 2400, Mol, Belgium
[c] Ghent University, Department of Soil Management, Research Group Soil Contamination, Coupure Links 653, 9000, Ghent, Belgium
[d] Ghent University, Department of Physics and Astronomy, Radiation Physics Research Group – Centre for X-ray Tomography (UGCT), Proeftuinstraat 86, 9000, Ghent, Belgium
[e] iFLUX, Science Park University of Antwerp, Galileilaan 15, 2845, Niel, Belgium
[f] University of Antwerp, Department of Bioscience Engineering, Groenenborgerlaan 171, 2020, Antwerp, Belgium

ARTICLE INFO

Keywords:
Marsh restoration
Groundwater flow
Macropores
Scheldt estuary
Controlled reduced tide (CRT)

ABSTRACT

In places where tidal marshes were formerly embanked for agricultural land use, these marshes are nowadays increasingly restored with the aim to regain important ecosystem services. However, there is growing evidence that restored tidal marshes and their services develop slowly and differ from natural tidal marshes in many aspects. Here we focus on groundwater dynamics, because these affect several key ecosystem functions and services, such as nutrient cycling and vegetation development. We hypothesize that groundwater dynamics in restored tidal marshes are reduced as compared to natural marshes because of the difference in soil structure. In the macro-tidal Schelde estuary (Belgium), in both a natural and a restored (since 2006) freshwater tidal marsh, we measured depth profiles of soil properties (grain size distribution, LOI (loss on ignition), moisture content and bulk density) and temporal dynamics of groundwater levels along a transect with increasing distance from a tidal creek. X-ray micro CT-scanning was used to quantify soil macroporosity. The restored marsh has a two-layered soil stratigraphy with a topsoil of freshly accreted sediment (ranging in depth between 10 and 60 cm, deposited since 2006) and a subsoil of compact relict agricultural soil. We found that both the soil in the natural marsh and the topsoil of the restored marsh consist of loosely packed sediment rich in macropores and organic matter, whereas the relict agricultural soil in the restored marsh is densely packed and has few macropores. Our results show that groundwater level fluctuations in the restored marsh are restricted to the top layer of newly deposited sediment (i.e. on average 0.08 m depth). Groundwater level fluctuations in the natural marsh occur over a larger depth of the soil profile (i.e. on average 0.28 m depth). As a consequence, the reduced groundwater dynamics in restored tidal marshes are expected to alter the subsurface fluxes of water and nutrients, the source-sink function and the development of marsh vegetation.

1. Introduction

Tidal marshes deliver many important ecosystem services: they play an important role in water quality regulation of adjacent estuaries and coastal areas (e.g. Barbier et al., 2011), carbon sequestration (e.g. Mcleod et al., 2011), mitigation of shoreline erosion and flood risks (e.g. Gedan et al., 2011) and they contribute to a large extent to the estuarine biodiversity (Costanza et al., 1997). During past centuries, however, many tidal marshes were embanked (i.e. reclaimed by building of flood defenses) and the soil was drained to gain land for agricultural, industrial or urban expansion (Bakker et al., 2002; Dijkema, 1987; Ma et al., 2014), leading to a loss of these ecosystem services. Within the framework of several legislations such as the EU Habitats and Water Framework Directive (European Parliament and the Council of the European Union, 2000), tidal marshes are increasingly restored on formerly embanked agricultural land (Blackwell et al., 2004; French, 2006; Wolters et al., 2005). The objective generally is that these restored tidal marshes develop relatively fast and deliver ecosystem services comparable to natural marshes. However, more and more studies show that restored tidal marshes and their ecosystem

* Corresponding author. University of Antwerp – Campus Drie Eiken, Ecosystem Management Research Group, Building C, room 1.27, 2610, Wilrijk, Belgium.
E-mail address: niels.vanputte@uantwerpen.be (N. Van Putte).

https://doi.org/10.1016/j.ecss.2019.02.006
Received 16 May 2018; Received in revised form 26 December 2018; Accepted 3 February 2019
Available online 16 February 2019
0272-7714/

functions and services develop slowly (e.g. Boorman and Hazelden, 2017; Garbutt and Wolters, 2008; Garbutt et al., 2006). Recently, it has been hypothesized that this slow maturation is linked to differences in subsurface hydrology between natural and restored marshes (Tempest et al., 2015), as subsurface groundwater fluxes are determining several ecosystem processes and services such as water quality regulation through nutrient cycling (Hughes et al., 1998; Nuttle, 1988) and vegetation development (Ursino et al., 2004). A thorough understanding of groundwater dynamics in restored versus natural tidal marshes is thus indispensable to propose new solutions to mitigate this problem in future marsh restoration plans.

Groundwater flow in tidal marsh soils was first described in the early work of Chapman (1938). A more advanced knowledge of subsurface hydrology in tidal marshes was only developed in the last decades and was to a large extent based on modeling or combined field and modeling studies (e.g. Gardner, 2005; Harvey et al., 1987; Hemond and Fifield, 1982; Moffett et al., 2012; Ursino et al., 2004; Wilson and Gardner, 2006; Xia and Li, 2012; Xin et al., 2011). For example, Harvey et al. (1987) illustrated the basic movement of groundwater in a salt-marsh soil: during the rising tide, intertidal creeks gradually fill and water infiltrates in the creek banks from the moment the surface water level in the creeks exceeds the groundwater table in the surrounding marsh soil. Around spring tides, the marsh platform inundates at high tide and surface water infiltrates into the marsh soil surface. During falling tide, the groundwater flows towards the creeks and seeps out of the creek banks, creating a hydraulic gradient towards the creeks. Tidally induced groundwater level fluctuations are the largest in the close vicinity of tidal creeks and dampen further in the marsh interior (Byers and Chmura, 2014; Ursino et al., 2004), where subsurface drainage is hindered and evapotranspiration is a major contributor for groundwater abstraction (Hemond and Fifield, 1982; Nuttle, 1988). Apart from the distance to the nearest creek, drainage is controlled by the permeability or hydraulic conductivity of the marsh soil (Montalto et al., 2006). Although the topsoil of many tidal marshes consists of fine grained, low permeable sediments, recent attention has been given to the presence of macropores (e.g. crab burrows and root channels), which might act as preferential flow paths for groundwater in marsh soils (Cao et al., 2012; Hughes et al., 1998; Susilo and Ridd, 2005; Xin et al., 2016).

Groundwater dynamics are controlling several key marsh ecosystem processes. As a result of tidally induced groundwater fluctuations, marsh sediments are intermittently saturated and unsaturated, inducing complex aeration conditions, hereby influencing plant development and the spatial distribution of marsh vegetation (Ursino et al., 2004; Xin et al., 2009, 2013). Impaired groundwater dynamics resulting in poor soil drainage may limit establishment and growth of marsh vegetation (Mendelssohn and Seneca, 1980). Furthermore, groundwater dynamics affect the soil redox status as more frequently saturated soils tend to exhibit more reduced conditions, which enhances the emission of methane (Byers and Chmura, 2014; Howes et al., 1981). In more aerated soils, on the other hand, microbial respiration leads to the emission of carbon dioxide (e.g. Heinsch et al., 2004). Therefore, groundwater dynamics influence the rate of carbon sequestration. Groundwater flow also induces solute exchange between the marsh soil and the surface water of adjacent estuaries or coastal areas, as pore-water seepage from creek banks exports substantial amounts of nutrients, such as dissolved silica (Struyf et al., 2007; Wilson and Gardner, 2006; Yelverton and Hackney, 1986). Especially flow in macropores enhances the advective flux of dissolved nutrients through marsh sediments (Harvey et al., 1995) and limits the diffusion and associated turnover of nutrients in the subsurface matrix.

When tidal marshes are converted to agriculture, for instance by dike building, soil drainage and associated soil aeration causes organic matter in the soil to decompose, leading to subsidence and compaction through consolidation of sediments (Brooks et al., 2015; Hazelden and Boorman, 2001; Portnoy, 1999; Spencer et al., 2008). The soil is often further compacted by the use of heavy farming equipment or trampling by cattle (Bantilan-Smith et al., 2009; Di Bella et al., 2015; Elschot et al., 2013; Nolte et al., 2013; Sloey and Hester, 2016). In saline soils, drainage can lead to soil dispersion, disintegrating the soil structure even more (Crooks and Pye, 2000). Restoring tidal marshes and their services on such historically compacted agricultural soils may therefore be hindered. Although many implications of soil compaction on developing restored tidal marshes have already been described (e.g. Sloey and Hester, 2016; Spencer et al., 2008), the link with subsurface hydrology is studied only to a limited extent.

Restored tidal marshes typically have a dual layered soil stratigraphy where the historical agricultural soil is overlain by sediment that was deposited since the reintroduction of the tidal regime, as is also the case in our restored site. Crooks and Pye (2000) suggested that compacted subsoils in tidal marshes might act as an aquaclude (i.e. an impermeable barrier for groundwater). The aim of this study is (i) to characterize both the compacted soil layer and the overlying layer of newly deposited sediment, (ii) to determine how these layers affect groundwater level fluctuations in a restored tidal freshwater marsh and (iii) how these groundwater level fluctuations differ from those seen in a natural freshwater tidal marsh. We hypothesize that soil properties (organic matter content, bulk density and macroporosity) changed because of the former agricultural land use, leading to a reduced permeability and reduced groundwater level fluctuations in the restored marsh compared to the natural marsh.

2. Methods and materials

2.1. Study site description

The study was conducted in the restored marsh “Lippenbroek” and the natural reference marsh “De Plaat”, described in Beauchard et al. (2011) and Vandenbruwaene et al. (2011), located in the freshwater tidal zone of the macro-tidal Scheldt estuary, Hamme, Belgium (51°05′ N, 4°11’ E, Fig. 1). The study sites are situated near the maximum tidal range of 4 m (neap tides) to 6 m (spring tides). Salinity varies between 0.5 and 0.75 (Jacobs et al., 2009). Meire et al. (2005) gives a more detailed description of the Scheldt estuary. The restored marsh site was, prior to the marsh restoration in 2006, an embanked agricultural area. Although the exact period of the embankment in Lippenbroek is unknown, large-scale land reclamation for agriculture in the wider area dates back from the 13th century. The elevation in the embanked site did not increase with a rising mean high water level in the river, as was the case in the natural marsh (Vandenbruwaene et al., 2011), and is therefore situated around 3 m lower than the natural marsh platform level. To obtain similar tidal conditions following restoration in the lower elevated agricultural area, the CRT (controlled reduced tide) approach was applied. In this system, the low elevated area is surrounded by a ring dike and water enters the area at high tide and leaves the area at low tide through a separate inlet and outlet sluice (Cox et al., 2006; Maris et al., 2007, Fig. 1), resulting in approximately 3 m lower high water levels in the CRT area compared to the estuary. During the embankment phase, parts of the site have been used for poplar (*Populus* sp.) plantations and in the last three decades before the restoration, an intensive crop rotation system with mainly maize (*Zea mays*) and potatoes (*Solanum tuberosum*) was established. During the phase of construction works needed for the restoration of tidal inundation (i.e. 2003–2006), the area was overgrown with a dense pioneer vegetation (mainly *Epilobium hirsutum* and *Urtica dioica*). Since the reintroduction of the tides in March 2006, this vegetation was outcompeted by typical low marsh vegetation (e.g. *Phragmites australis, Typha latifolia, Bolboschoenus maritimus* and *Lythrum salicaria*) and willow trees (*Salix* spp.) on the higher elevated parts (Jacobs et al., 2008). The natural marsh is located at the riverside of the dike approximately 1 km upstream from the inlet/outlet structures of the CRT area (Fig. 1). At the study location, the dominant plant species are willow trees, *Impatiens glandulifera*

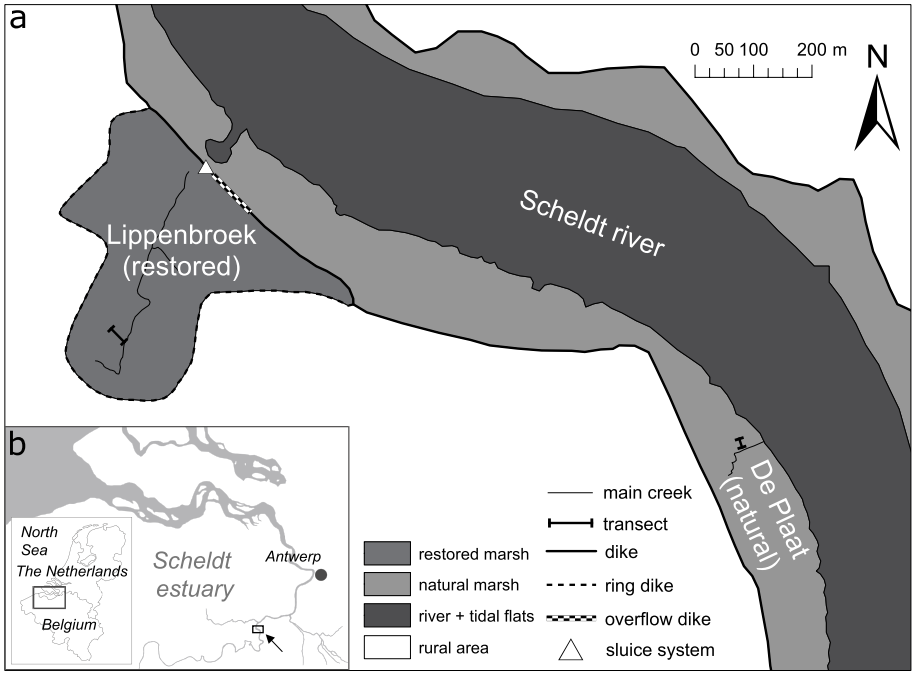

Fig. 1. (a) Overview map of the study area, (b) situation of the study area in the Scheldt estuary (indicated with an arrow) and situation of the Scheldt estuary in Belgium and The Netherlands.

and *Urtica dioica*.

In both the natural and restored marsh sites, the top layer of the sediment is a typical marsh soil with high amounts of silt (Fig. 2). In the restored site, the sediment deposited after the reintroduction of the tides, rests on top of an approximately 2 m thick layer of relict agricultural soil, of which especially the upper part is heavily compacted. This fine grained Holocene sediment is underlain by more sandy Pleistocene sediment, including glauconite and pieces of peat. The soil stratigraphy in the natural marsh follows a typical fining upwards pattern (e.g. O'Connor and Moffett, 2015) with over 60% of sand below 3 m depth (Fig. 2a).

2.2. Experimental design

All the data were collected on a transect approximately perpendicular to a tidal creek with a similar depth of approximately 1 m (see locations on Fig. 1). This design is based on insights from literature on subsurface hydrology in tidal marshes, which state that groundwater level fluctuations and fluxes are related to the distance from tidal creeks (e.g. Gardner, 2005; Montalto et al., 2007; Ursino et al., 2004; Wilson and Gardner, 2006; Xin et al., 2013). We installed five groundwater monitoring wells with an inner diameter of 41 mm, separated 5 m and 8 m from each other in the natural and the restored marsh, respectively (Fig. 3). A shorter transect was made in the natural marsh for the reason that any longer transect would intersect other nearby creeks. The transect in the natural marsh was located approximately 25 m inland from steep erosion cliffs that delineate the border between the marsh and the tidal flats. The first monitoring well on both transects was placed at approximately 1 m from the creek edge. The entire subsurface part of the wells was screened. Filter sand was applied in a gauze around the wells and the boreholes were sealed off from the surface with a 5 cm thick bentonite seal. In the restored marsh wells, a second bentonite seal was applied between the relict agricultural polder soil and the newly deposited sediment to prevent preferential flow between the two layers (Fig. 3c). Pressure transducers (Mini Diver®) measured the groundwater level in the wells at an interval of 2 min over an almost 6 months period from October 23rd, 2015 to March 16th, 2016, covering approximately 10 spring tide – neap tide cycles. Measured groundwater level data were corrected for atmospheric pressure variations with data from a nearby weather station (www.meteomoes.be), located between 1 and 2 km from the study sites. Due to the different correction steps that are needed to obtain the absolute groundwater level, deviations of a few cm from the true value are possible. As the dataset mostly covers the winter period when the marsh platform is unvegetated, but covered with plant detritus, the effect of evapotranspiration on the groundwater level was not considered in this study. Surface water level data were obtained from the Flanders Hydraulics Research (Waterinfo, 2016). The absolute elevation of the monitoring wells and the topographic surface profile of the transects, including the creek profile, were measured with an RTK-DGPS and are presented in m TAW (the Belgian ordnance level, which at the measuring location corresponds approximately to the mean low water level). To estimate the thickness of the deposited sediment layer in the restored marsh, we took soil cores with a small gouge auger next to the monitoring wells. The soft newly deposited sediment could easily be removed from the gouge, while the underlying relict agricultural soil is compact and therefore tightly fixed in the gouge. As such, the newly deposited sediment and underlying relict agricultural soil could be clearly

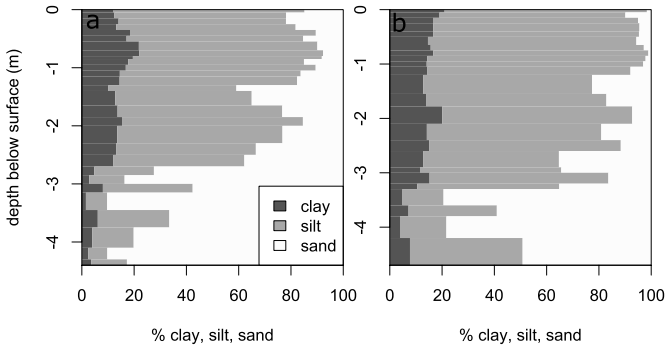

Fig. 2. Overview of the volumetric grain size fractions (clay, silt and sand, on the scale of Wentworth (1922) and Udden (1914) for a soil profile in (a) the natural and (b) the restored marsh, respectively. Depths are expressed relative to the soil surface.

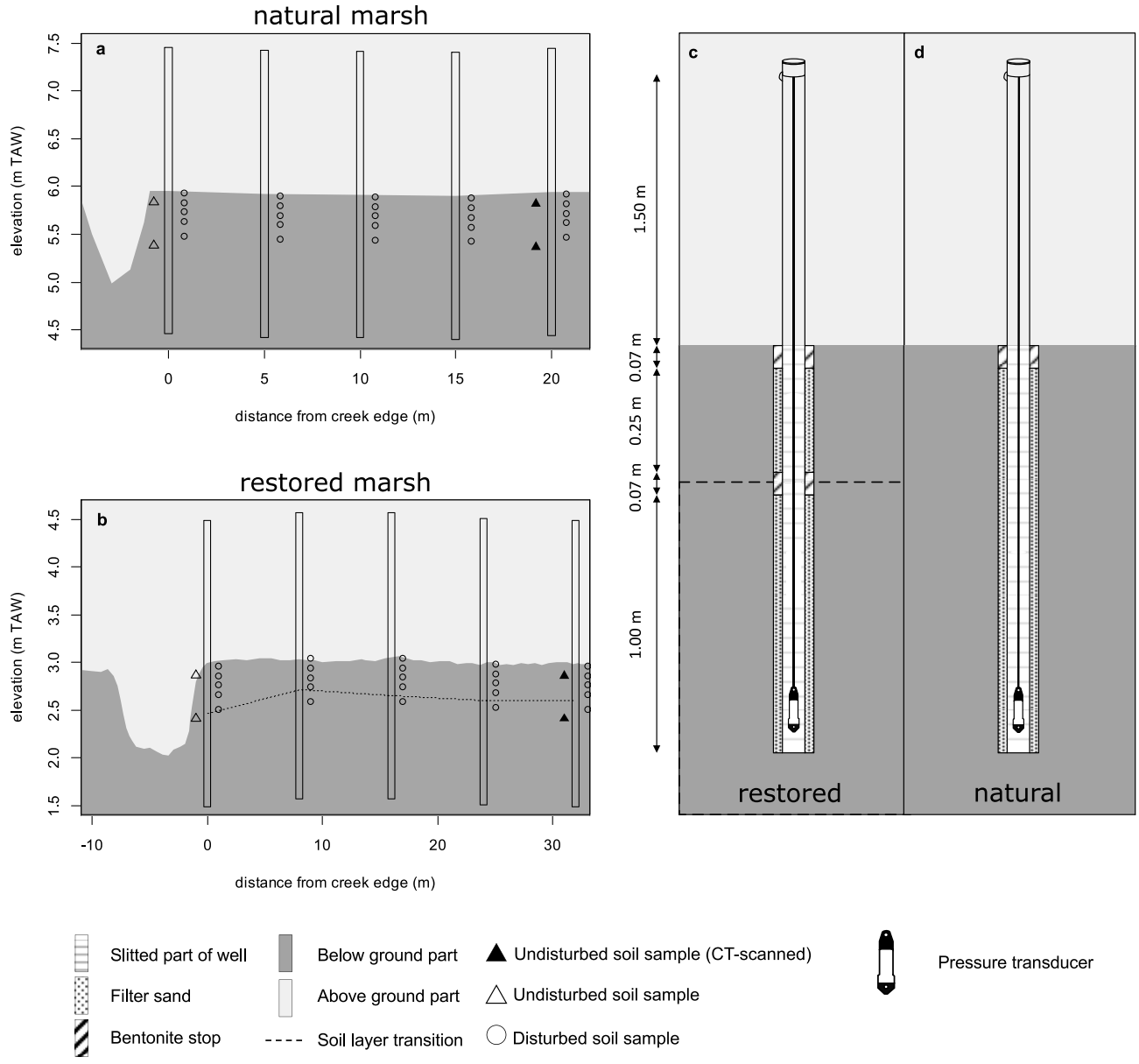

Fig. 3. Experimental set-up and sampling locations drawn on a cross section of the creek and the marsh platform for (a) the natural marsh and (b) the restored marsh. All soil samples were taken in triplicates. Vertical bars represent the monitoring wells. The design of the monitoring wells is presented in detail in (c) for the restored marsh and (d) for the natural marsh.

distinguished and the distance between the surface level and the soil layer transition was measured with a folding rule.

Around each well on the transects, three disturbed soil cores were taken with a 5 cm wide gouge auger (Fig. 3a and b). Each core was subsampled into five depth ranges (0–5 cm, 10–15 cm, 20–25 cm, 30–35 cm and 45–50 cm). Around the first and the last monitoring well on the transects (later referred to as the 'near-creek zone' and 'marsh interior', respectively), three undisturbed soil samples were taken between 10 cm and 15 cm depth (i.e. corresponding with the tidally deposited upper sediment layer in the restored marsh) and three samples between 55 cm and 60 cm depth (i.e. corresponding with the deeper former agricultural soil in the restored marsh). To minimize compaction and soil disturbance, a borehole was made with an Edelman auger to the desired depth and the bottom of the borehole was leveled with a Riverside auger, after which the undisturbed soil sample was excavated using a sample ring kit with open ring holder. To allow analysis of these samples with computed tomography (see further), we used custom-made, sharp edged PVC sample rings with a height of 50 mm and an inner diameter of 45 mm. All samples were cooled before analyses at 4 °C.

2.3. Micro-CT scanning of soil cores

To assess the distribution of macropores and organic matter in the marsh soil, the twelve undisturbed soil samples taken in the marsh interior in both areas were imaged using high-resolution X-ray CT scanning (μCT). This non-destructive technique allows to visualize and analyze the structure of the object in 3D (Cnudde and Boone, 2013). The scans were performed at the HECTOR system of the Ghent University Centre for X-ray Tomography (UGCT) described in Masschaele et al. (2013), using a tube voltage of 140 kV. The resulting datasets contained approximately 1 gigavoxel (1000^3) at an isotropic voxel (i.e. 3D pixel) size of 60^3 μm^3. The grey value for each voxel represents the local X-ray attenuation coefficient, which depends on both the chemical

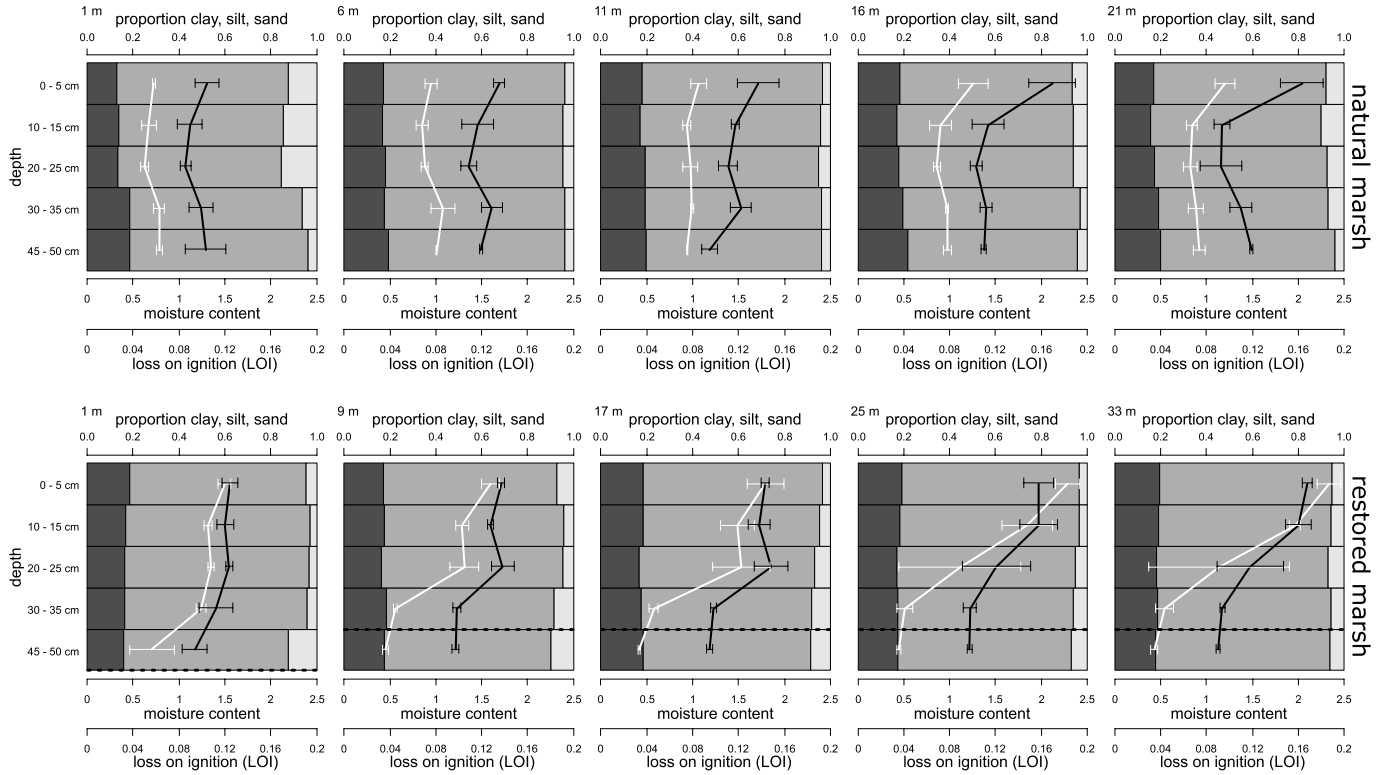

Fig. 4. Soil properties along the transects in the natural marsh (upper panels) and the restored marsh (lower panels) as a function of the depth and distance from the creek edge (indicated in the upper left corner of each graph). Dark grey, intermediate grey and light grey bars represent the volumetric proportions of clay, silt and sand, respectively. White lines represent the gravimetric moisture content and black lines represent the loss on ignition (LOI) as a fraction. Horizontal dashed lines indicate the approximate location (rounded to the nearest sampling interval) of the transition from newly deposited sediment to compacted subsoil. Error bars indicate the standard deviation (n = 3).

composition and density of the material. Based on the grey value histogram of the complete dataset of all scanned soil cores, threshold values were manually defined and the grey values were segmented using Octopus Analysis® (Brabant et al., 2011; Vlassenbroeck et al., 2007) in one of the following categories: air filled macropores (linear attenuation coefficients $< 0.16\,cm^{-1}$), organic matter or water filled macropores ($0.16\,cm^{-1} - 0.40\,cm^{-1}$) and mineral sediment ($> 0.40\,cm^{-1}$). Due to a similar X-ray attenuation, resulting in a similar grey value, water filled macropores and organic matter could not be distinguished. As a result of the partial volume effect, the grey value of each voxel is proportional to the weighted average of the linear attenuation coefficient of the different constituents present within that voxel (Barrett and Keat, 2004). Therefore, voxels containing both mineral sediment and air filled macropores have an intermediate value, which might be in the defined attenuation range of organic matter. After thresholding, voxels that were erroneously classified as a result of noise or partial volume effects were removed by applying the binary operations closing and opening (Brabant et al., 2011; Soille, 1999). The 150 first and last images (along the z-axis = depth profile) of each sample were not used in the analyses because they displayed aberrations which were due to both cone beam artefacts in the CT scans (e.g. Barrett and Keat, 2004) and disturbance of the sample edges while taking the samples (accidental smearing when removing excess sediment protruding from the sample rings). 3D renderings of the sediment, organic matter and macropore fractions were made using VGSTUDIO MAX 3.2 (http://www.volumegraphics.com, Fig. 6).

2.4. Lab analyses

A subsample of each disturbed soil sample was used to determine the volumetric grain size distribution with a Mastersizer 2000 (Malvern Instruments Ltd.) based on laser diffraction after treatment with HCl and H_2O_2 to remove organic matter. The fraction of clay, silt and sand in the samples was determined on the scale of Udden (1914) and Wentworth (1922) (clay: < 4 µm, silt: 4–63 µm, sand: 63–2000 µm). The remainder of the samples was dried at 70 °C for at least 48 h to determine the gravimetric moisture content (weight loss/dry mass). As samples in both marshes were taken on different days, moisture content cannot be directly compared between both areas. The gravimetric organic matter content in the samples was estimated with the loss on ignition (LOI) method (e.g. Heiri et al., 2001) with a muffle furnace at a temperature of 550 °C.

After CT-scanning, the vertical saturated hydraulic conductivity of the undisturbed soil samples was measured with a laboratory permeameter in which water seeps through undisturbed soil samples placed in a container filled with water (Eijkelkamp Agrisearch Equipments, 2013). We used the constant head method for samples with a saturated hydraulic conductivity higher than 1 cm/day, whereas we used the falling head method for samples with a lower hydraulic conductivity. The aim of these measurements was to test the relation between macroporosity and hydraulic conductivity for individual samples, rather than to obtain an accurate value for the field hydraulic conductivity. Bulk density was determined as dry mass (105 °C, > 48 h) over total volume.

2.5. Data analyses

All statistical analyses were performed in R (R Development Core Team, 2015) and tidal characteristics (inundation time and frequency) were determined using the 'Tides' package (Cox, 2017).

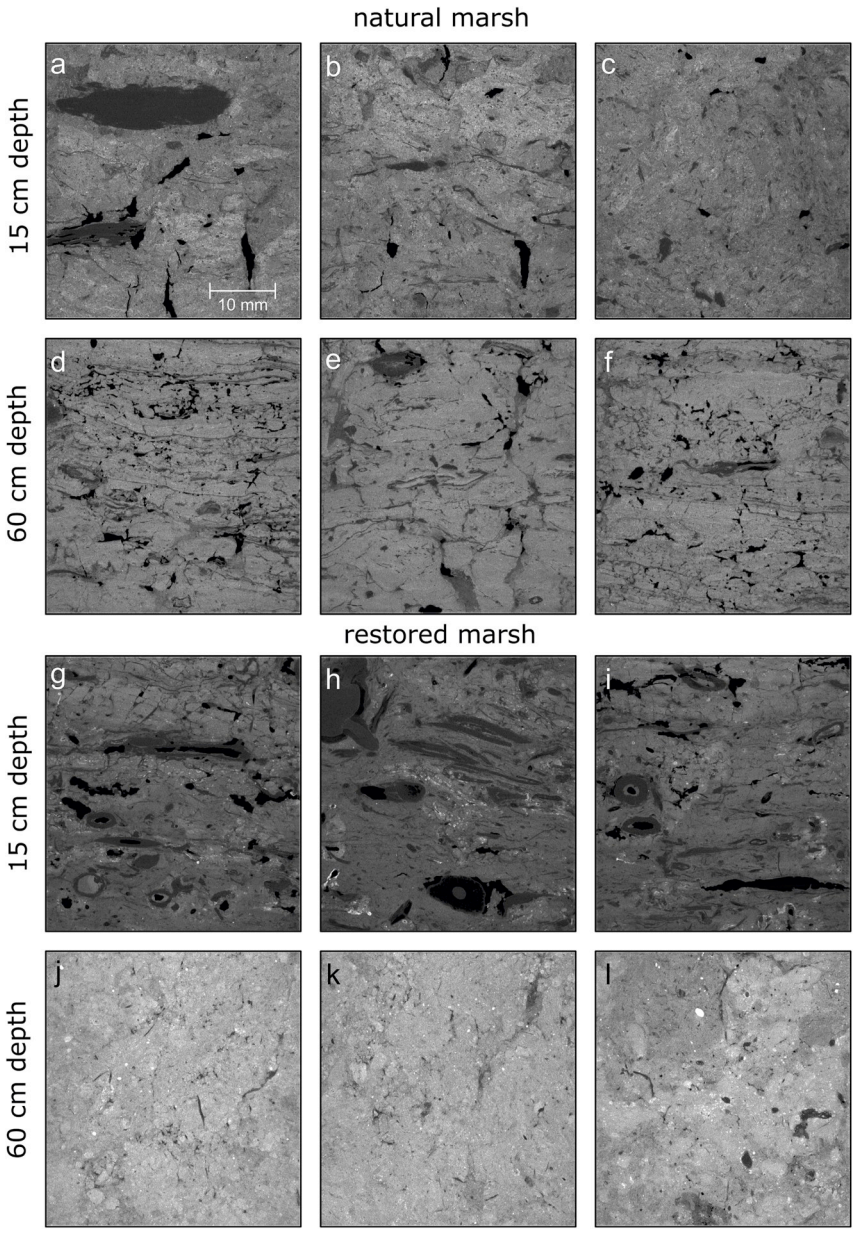

Fig. 5. CT-scan images of all the undisturbed soil samples taken in the marsh interior. Brighter areas represent denser sediment. Dark grey areas represent organic matter or water-filled macropores, black areas represent air-filled macropores. The images show a vertical cross section through the middle of each sample.

3. Results

3.1. Soil characteristics

3.1.1. Grain size distribution, gravimetric moisture content and organic matter content

Grain size distribution (soil texture) and organic matter content strongly control water retention in soils. In the natural marsh, a higher proportion of sand is observed close to the creek (Fig. 4). Only in the upper 5 cm, there is an increasing soil moisture and LOI with an increasing distance from the creek. Below 5 cm, neither grain size distribution nor moisture and LOI show a clear change in function of depth or distance from the creek. In contrast, in the restored marsh, two distinct soil layers can be discerned. The upper layer consists of loosely packed sediment that was deposited since the first inundation of the marsh in 2006. Over the transect, this layer has a thickness of 39 ± 4 cm in the marsh interior and 52 ± 4 cm at 1 m from the creek. In the upper 15 cm, the organic matter and moisture content increase with an increasing distance from the creek. Below 30 cm, in the relict agricultural soil, both the LOI and moisture content are relatively constant and low.

3.1.2. Bulk density, macroporosity and saturated hydraulic conductivity

Fig. 5 presents CT-scan images from soil cores in both areas. Assuming that the mineral fraction has an identical composition in both areas, which is reasonable as the sediment in both areas originates from a common source, brighter colors indicate denser packed sediment particles, i.e. a lower degree of microporosity (Cnudde and Boone, 2013; Spencer et al., 2017). Visual assessment of these images and 3D renderings of the different components (Fig. 6), revealed that the sediment in the natural marsh is intersected by pieces of wood, roots and macropores both at 15 and at 60 cm depth. Some of these macropores have the shape of cracks or fissures, whereas others are more irregularly or tubular-shaped. In the newly deposited sediment of the restored marsh (at 15 cm depth), hollow plant structures, such as roots or stems from marsh vegetation, were clearly visible on the CT-scan images, as

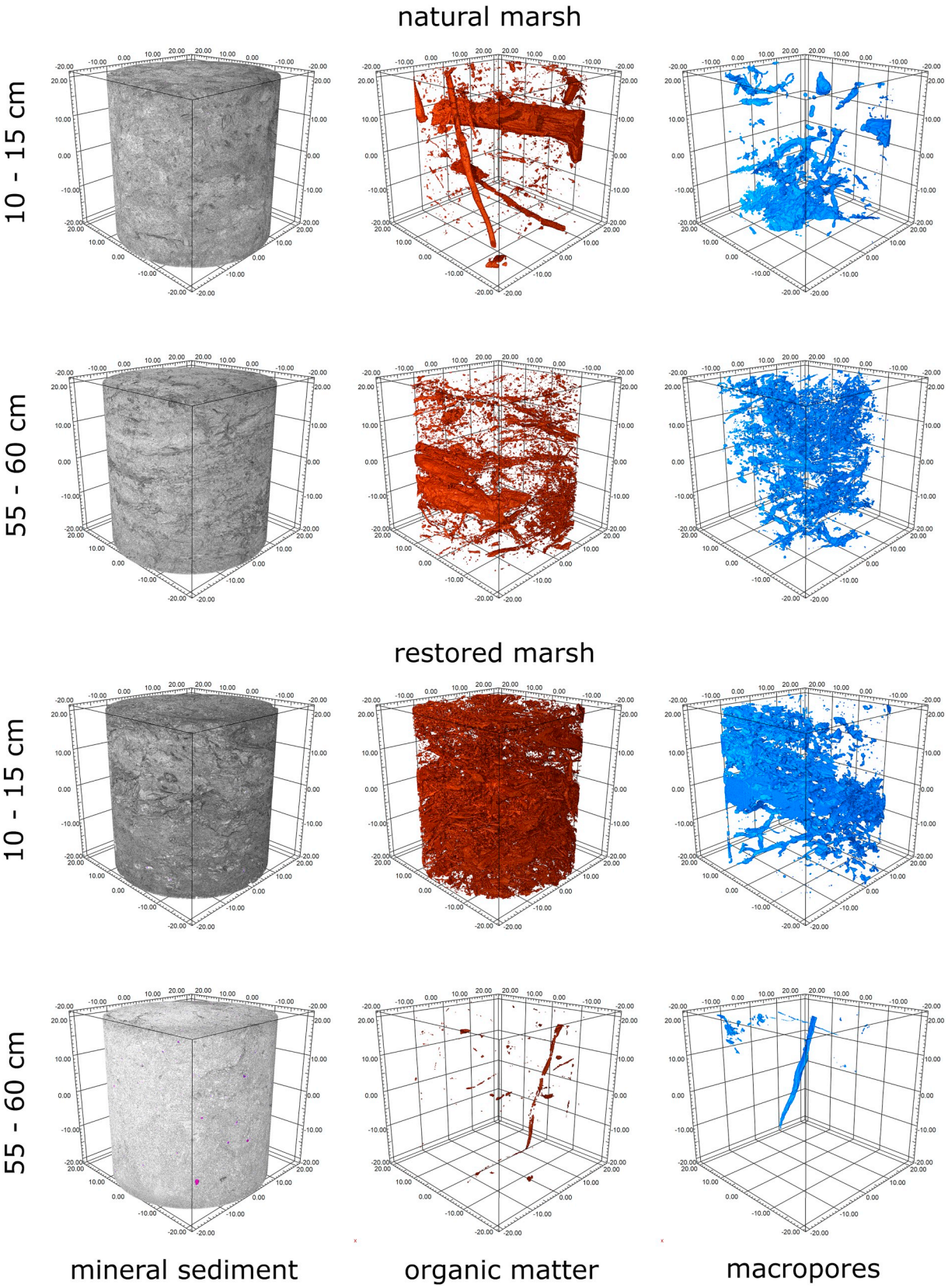

Fig. 6. 3D renderings of the fractions of mineral sediment, organic matter and macropores for one of the triplicate samples taken in the marsh interior of both study sites. In the renderings of the mineral sediment, lighter areas represent more dense sediment. Very high density mineral inclusions are represented in purple. Labels on the axes are in mm. (For interpretation of the references to color in this figure legend, the reader is referred to the Web version of this article.)

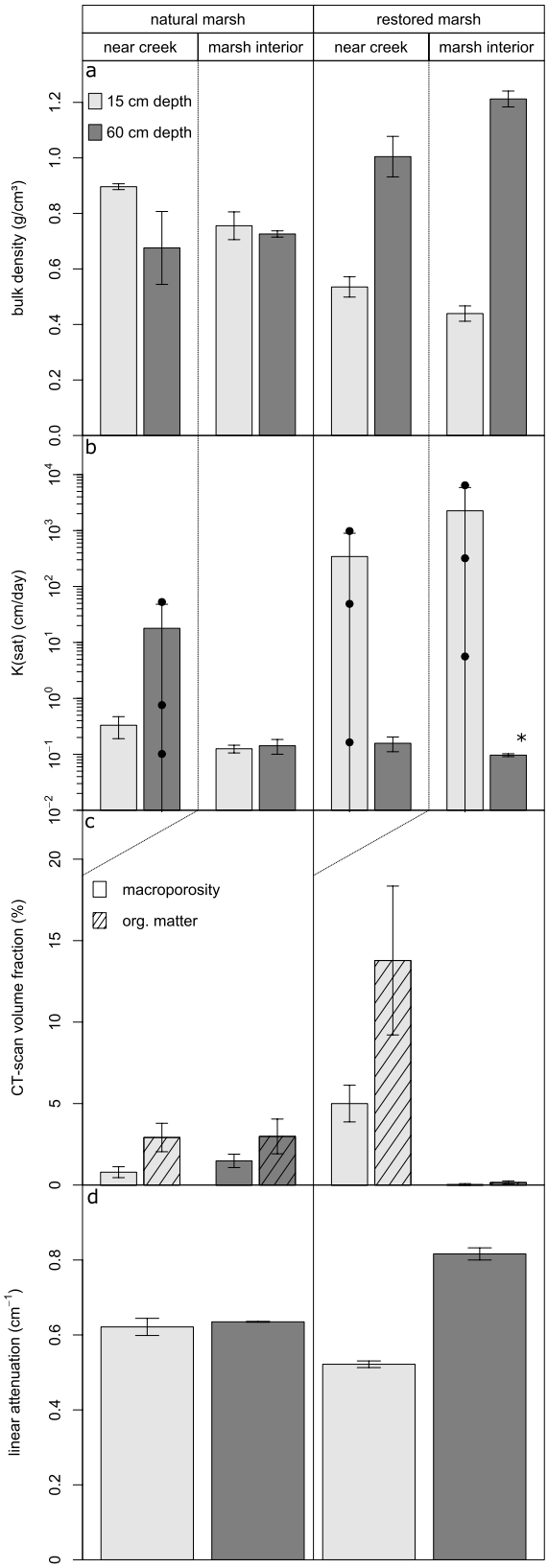

Fig. 7. comparison of soil properties measured on undisturbed soil samples from both the natural and the restored tidal marsh in function of depth and location in the marsh. Values are displayed as mean ± standard deviation (n = 3). (a) dry bulk density (b) saturated hydraulic conductivity. Note that the y-axis is logarithmic. Where the variation between the triplicates was several orders of magnitude, the individual measurement values are plotted as well (black bullets). *: actual value was lower than could be accurately measured with the lab permeameter. (c) volume fraction of air filled macropores and organic matter/water filled macropores. The latter could not be distinguished due to a similar X-ray attenuation. (d) Linear attenuation coefficient of the sediment phase. Note that CT-scans were only performed on samples taken in the marsh interior.

well as large irregular and tubular void spaces (Fig. 5g, h, i, Fig. 6). In the underlying relict agricultural soil (at 60 cm depth), only few small tubular and spherical macropores were present (Fig. 5j, k, l, Fig. 6). In both the natural and restored marsh areas, the creek banks are pierced by large holes (with diameters of several cm) that are presumably old root channels or burrows of the Chinese mitten crab (*Eriocheir sinensis*). Some of these holes have been observed to drain considerable amounts of water to the tidal creeks at low tide. Just above the compacted soil, a zone with large water filled macropores was observed. We hypothesize that this is a relic of a former ploughing layer.

For the natural marsh, an ANOVA revealed no significant difference between the volume fraction of air filled macropores nor the volume fraction of organic matter/water filled macropores for samples taken at 15 cm depth and 60 cm depth (Fig. 7c, Table 1). We did find a significant difference between bulk density of the samples ($F_{1,8} = 9.39$, $p = 0.0155$). A Tukey's HSD *post hoc* test indicated that bulk density at 15 cm depth is on average 0.13 g/cm^3 higher than the bulk density at 60 cm depth (Fig. 7a). In the restored marsh, both the volume fraction of air filled macropores and the volume fraction of organic matter/water filled macropores are significantly higher in the newly deposited sediment (15 cm depth) than in the compacted subsoil (60 cm depth, Fig. 7c, Table 1). Bulk density at 15 cm depth is on average 0.62 g/cm^3 lower than at 60 cm depth ($F_{1,8} = 562.20$, $p < 0.0001$, Fig. 7a). This is also reflected in a significantly higher linear attenuation coefficient (i.e. a lower degree of microporosity, Fig. 7d, Table 1). The saturated hydraulic conductivity of the layer of newly deposited sediment in the restored marsh is very variable, and several orders of magnitude higher compared to both the compacted agricultural soil in the restored marsh, and the soil in the natural marsh (Fig. 7b).

3.2. Subsurface hydrology

As a result of the different elevation and the CRT design (see before), the natural and the restored marsh exhibit different inundation characteristics (Fig. 8), as explained in Cox et al. (2006). During the measured time span, the studied region in the natural marsh was flooded in 36% of all tides and the average inundation time was 79 min, whereas the studied region in the restored marsh was flooded during 76% of all tides with an average inundation time of 276 min.

The natural and the restored marsh also showed a remarkably different pattern in groundwater dynamics. In between consecutive

Table 1
Significance table for macroporosity, organic matter content and linear attenuation coefficient of the sediment phase based on CT-scan data that are presented in Fig. 7. For both sites, a comparison is made between samples taken at 15 cm depth and 60 cm depth (n = 3). Based on a one-way ANOVA.

	Air macropores		Organic matter		Linear attenuation	
	$F_{1,4}$	p	$F_{1,4}$	p	$F_{1,4}$	p
Natural marsh	5.149	0.086	0.007	0.938	1.050	0.3634
Restored marsh	58.167	0.002	26.674	0.007	761.050	< 0.001

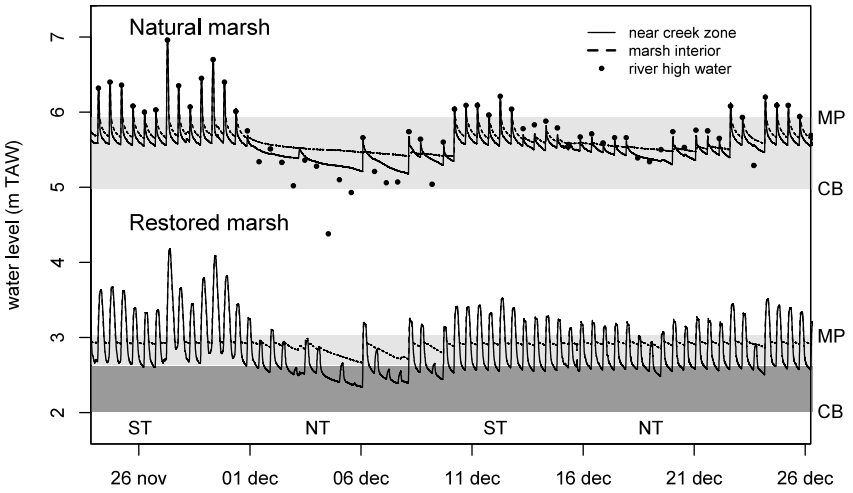

Fig. 8. Water level measured in the monitoring wells in the natural marsh and the restored marsh for a period from November 26, 2015 to December 26, 2015 covering two spring tide (ST) – neap tide (NT) cycles. The grey shaded areas represent the elevation range between the creek bottom (CB) elevation and the average marsh platform (MP) elevation, with the dark grey part representing the old agricultural polder soil and the light grey part the deposited sediment. Note that the high water level in the restored marsh does not correspond to the high water level in the estuary as a result of the CRT design (see text).

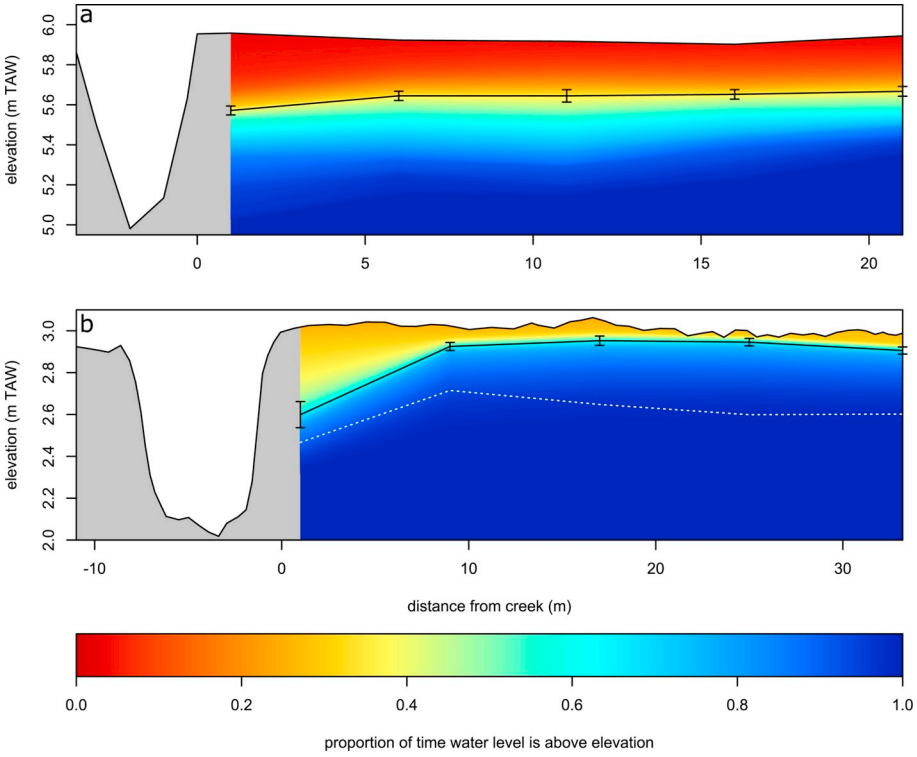

Fig. 9. Cross section of the creek and marsh platform for (a) the natural marsh and (b) the restored marsh. Colors represent the proportion of time that the groundwater level was above the corresponding elevation on the y-axis. The colored region is restricted to the transect where the measurements took place and values are linearly interpolated between the five measuring points. Black lines represent the mean lowest groundwater level between two consecutive inundating tides. Error bars represent the standard deviation of these values. The dotted white line in the restored marsh (b) indicates the approximate location of the transition between the compact agricultural soil and the newly deposited sediment. (For interpretation of the references to color in this figure legend, the reader is referred to the Web version of this article.)

inundating tides (determined here as two high tides that inundate the marsh platform and are separated less than 15 h in time), the groundwater level in the natural marsh fell on average 28 cm below the marsh platform in the marsh interior and 36 cm in the near creek zone (Fig. 9a). In the restored marsh, the decline in groundwater level in between consecutive inundating tides was on average only 8 cm below the platform in the marsh interior and 41 cm near the creek. The lowest groundwater level during neap tide was very much depending on the number of consecutive non-inundating tides (Fig. 8). Over the measured timespan, the minimum-recorded groundwater level in the natural marsh was 72 cm below the surface averaged over the marsh interior and 94 cm near the creek. The minimum groundwater level in the restored marsh was 49 cm below the surface averaged over the marsh interior and 67 cm near the creek. In the restored marsh, the groundwater level is above the transition between the newly deposited sediment and the compact relict agricultural soil for at least 90% of the measured time (Fig. 9b). Thus, groundwater level fluctuations occur over a deeper soil profile in the natural marsh compared to the restored marsh.

During non-inundating tides, i.e. high tides that inundate the intertidal creeks but that do not flood the vegetated marsh platform, the groundwater table in the natural marsh rises when water fills the tidal creeks (Fig. 8). This rise is most prominent close to the creek and less so further into the marsh interior. In the restored marsh, only the water level in the monitoring well next to the creek noticeably reacts to a rising water level in the creek. During inundating tides, the water level in all the monitoring wells in both areas rises quickly and simultaneously with the surface water level from the moment the marsh starts flooding. When the surface water recedes from the marsh platform, the water level in the wells decreases approximately logarithmic over time (Fig. 8). The groundwater level in both the natural and the restored marsh drops faster close to the creek and slower further away from the creek, so that over time a hydraulic gradient develops towards the creek. In the natural marsh, this hydraulic gradient extends throughout

the entire transect, whereas the hydraulic gradient in the restored marsh is larger and is only present in the vicinity of the creek (Fig. 8 and 9b). After the last inundation before neap tide, the hydraulic gradient in the natural marsh becomes steeper. In the restored marsh, the decrease in groundwater level then occurs more equally along the transect. When the groundwater table approximates the underlying relict agricultural soil in the restored marsh, the decrease in groundwater level attenuates (Fig. 8 and 9b).

4. Discussion

Tidal marshes are increasingly restored on formerly embanked agricultural land to regain important ecosystem services, such as habitat provisioning and nutrient cycling, which are depending on groundwater dynamics and hence soil conditions. This study has shed new light on differences in physical soil properties (including macroporosity) and groundwater dynamics between a natural and a restored freshwater tidal marsh in the Scheldt estuary. Historical land-use in formerly embanked areas has often resulted in altered soil properties that may constrain the groundwater dynamics after marsh restoration. Even after decades, restored tidal marshes often differ significantly from their natural counterparts concerning e.g. vegetation composition and biogeochemical functioning (e.g. Boorman and Hazelden, 2017; Brooks et al., 2015; Craft et al., 1991; Garbutt and Wolters, 2008; Mossman et al., 2012; Spencer et al., 2008). Although the notion that both vegetation development and nutrient cycling are strongly related to subsurface hydrology is well established for natural tidal marshes (e.g. Hughes et al., 1998; Nuttle, 1988; Wilson et al., 2015), only few papers (e.g. Montalto and Steenhuis, 2004; Tempest et al., 2015) have studied subsurface hydrology in restored tidal marshes in comparison to natural reference marshes. Our results indicate that groundwater level fluctuations occur over a deeper soil profile in the natural marsh compared to the restored marsh, where subsurface drainage is hindered by the compact relict agricultural soil, underlying the newly deposited sediment. Although the soil in the restored marsh has comparable texture in both layers, CT-scans and bulk density analyses showed that the soil in the lower agricultural soil layer is denser packed and has a significantly lower macroporosity and microporosity, a higher bulk density and lower LOI than the upper newly deposited sediment layer. Hence, both vertical and lateral groundwater fluxes are restricted to a smaller, less deep portion of the soil profile in the restored marsh.

4.1. Changed soil properties as a result of agricultural land use

Both the soil in the natural marsh and the upper layer of the restored marsh consist of macropores and pieces of organic matter embedded in a fine grained (mostly silt) sediment matrix. By contrast, only few small macropores are present in the relict agricultural soil. Contrary to our results, a recent study of Spencer et al. (2017) in SE England found a higher macroporosity with higher connectivity of macropores in the relict agricultural soil of a restored saltmarsh (after so-called managed realignment) compared to the layer of newly deposited sediment and the soil in a nearby natural saltmarsh. The micro-CT scans in their study contain data on a soil profile of 7.4 cm depth with the upper 4 cm being the newly deposited sediment. Hence, in that study the agricultural soil was sampled and analyzed directly beneath the newly deposited sediment, which might be in a relict macroporous ploughing layer (Spencer et al., 2017). We studied the macroporosity at 55–60 cm depth, which is much deeper and is considered to exist below such a ploughing layer.

Macropore networks play a very important role in marsh subsurface hydrology as they form preferential flow paths through which water can infiltrate (Hughes et al., 1998) and drain (Xin et al., 2009). As a result, macropore networks increase the hydraulic conductivity of the soil, especially in otherwise low permeable sediments (Montalto et al., 2006). In our study, this was apparent in the upper layer of the restored marsh (Fig. 7). Nevertheless, a relatively low hydraulic conductivity was measured in the samples from the natural marsh, despite the relatively high macroporosity. This observation does not correspond to the fast decline of water levels in the wells after the tide recedes (Fig. 8). In our set-up for measuring hydraulic conductivity, only macropore networks that intersect both the top and bottom of the sample might significantly affect the hydraulic conductivity measured with a lab permeameter.

Natural freshwater tidal marshes are built up of sediment that was deposited by the tidal water over hundreds of years. Together with the mineral sediment, organic matter is deposited and gets buried within the soil (Kadiri et al., 2011). During the low water phase, the groundwater table in the marsh declines, inducing soil aeration (Xin et al., 2010). As a consequence, buried organic material is partly decomposed, resulting in the formation of macropores (Beven and Germann, 1982). Due to the increased soil aeration, more favorable conditions for plant growth (Ursino et al., 2004) and soil biota (Beauchard et al., 2013; Schmitz and Harrison, 2004) can develop, leading to a positive feedback loop (Luo et al., 2010; Tempest et al., 2015; Ursino et al., 2004; Xin et al., 2013) as decayed plant roots and burrowing invertebrates create new macropores. Harvey et al. (1995) found that the volume of macropores in the soil corresponds to the proportion of soil volume in which solute transport occurs and that nutrient concentrations can be three times higher in matrix pores compared to macropores, suggesting fast flushing of dissolved nutrients through macropore networks. Large macropores (e.g. crab burrows) in creek banks, as also observed in both of our field sites, can be responsible for faster groundwater level fluctuations near the creek banks (Montalto et al., 2006).

Tidal marshes are typically restored on low lying agricultural land that has been subjected to extended periods of drainage and subsequent subsidence and compaction of the soil, as organic matter is further mineralized (Iost et al., 2007) and, more recently, heavy farming equipment is used (Bantilan-Smith et al., 2009; Sloey and Hester, 2016), to which macropore networks are extremely vulnerable (Beven and Germann, 2013). For saltmarshes, Crooks and Pye (2000) add that in carbonate deficient soils, the soil fabric may totally collapse when clay particles disperse after drainage of the saline soil. In our freshwater study sites, this effect is expected not to play a role. Our study provides further indication that original marsh soil properties are not reversed in a reasonable time frame after the reintroduction of the tidal regime, with major implications for subsurface hydrology.

4.2. Reduced groundwater fluctuations in the restored tidal marsh

Tidally induced groundwater fluctuations in the restored marsh are restricted to the layer of newly deposited sediment, supporting the conclusions of Tempest et al. (2015) that the compacted soil, underlying this layer, acts as a barrier for groundwater flow. Furthermore, the groundwater level only approximates the transition of the soil layers (which is located at approximately 40 cm depth) during extended periods without inundations (i.e. around neap tides). In between consecutive inundating tides, the groundwater level in the marsh interior does not decline to more than 10 cm below the marsh platform. Close to the creek (< 1 m), the groundwater level drops deeper after the tide recedes and rises with a rising surface water level in the creek, even during non-inundating tides. We can therefore expect that, in accordance to the findings of Wilson and Gardner (2006) for numerical simulations of a natural tidal marsh, the majority of seepage to creeks originates from groundwater within the first few meters from the creek edge. This underpins the importance of a dense creek network for the aeration and biogeochemical cycling of restored tidal marsh soils. However, compacted soil layers can hamper the incision of creek networks (Vandenbruwaene et al., 2012), possibly further reducing the capability of the marsh to increase its drainage capacity after restoration.

Groundwater level fluctuations in the natural marsh were also strongest close to the creek and weaker further in the marsh interior,

but a remarkable decline in groundwater level was still observed at 21 m from the creek, which is further than described in most studies (e.g. Nuttle, 1988) who found that tidally induced groundwater drainage is negligible in a marsh soil further than 15 m from the creek. This may partly be the result of exfiltration through the steep erosion cliffs that mark the edge of the tidal marsh towards the tidal mudflats, as our transect was situated around 25 m from this approximately 1 m high cliff. As mentioned above, the observed groundwater level decrease after inundation in the natural marsh was faster than could be expected based on the measured vertical saturated hydraulic conductivity. This suggests a more complex situation where groundwater mainly flows through larger scale macropore networks that may not have been contained in our soil samples.

In this paper we focused on fluctuations of the groundwater table. However, in the fine grained soil of both the natural and the restored tidal marsh, a thick capillary fringe is likely to be present above the groundwater table (Kong et al., 2015). Where this groundwater table is shallow, as observed in the restored marsh, the capillary fringe can extend to the soil surface (Drabsch et al., 1999), limiting soil aeration and surface water infiltration, and promoting pore water removal by evaporation (Xin et al., 2017). In order to fully understand the subsurface hydrology of restored tidal wetlands, the capillary fringe and the overlying vadose zone should be considered as well. This requires measurements of soil water potential or water content and/or numerical simulations in a variably saturated porewater model.

4.3. Implications of reduced groundwater dynamics for ecosystem functioning

A slow development of soil properties and subsurface hydrology can have major implications for the ecosystem functions and services of restored wetlands, which are often targeted and expected to develop within a certain timeframe (Ballantine et al., 2015). Plant communities in restored tidal marshes have to cope with higher average groundwater levels and therefore may differ from plant communities observed in natural tidal marshes (Brooks et al., 2015; Wolters et al., 2005). These higher groundwater levels reduce the soil aeration depth. It must, however, be noted that in tidal marshes with a low hydraulic conductivity (< 8.64 cm/day $= 10^{-6}$ m s^{-1}), an unsaturated zone can persist below the surface even during inundation (Byers and Chmura, 2014; Ursino et al., 2004). Moreover, vegetation oxidizes the sediment in the root zone (Howes et al., 1981; Kolditz et al., 2009). Besides the direct effect on groundwater levels, the compact agricultural soil can also form a barrier for plant roots (Brooks et al., 2015) and burrowing species (Tempest et al., 2015; Xin et al., 2009), restricting the formation of macropores and thus hindering a development towards an increased soil drainage capacity. Furthermore, groundwater dynamics control several geomorphological processes. In restored tidal marshes, impaired drainage hampers consolidation of the newly deposited sediment and hence leads to a low dry bulk density of this sediment, resulting in a faster increase of the marsh platform elevation with an equal sediment mass accumulation rate. On the other hand, the less consolidated sediment has a lower bulk density and is therefore expected to have a lower shear strength and to be more vulnerable to erosion (Crooks and Pye, 2000).

Despite these adverse effects that reduced groundwater drainage can have on marsh development, a fast development of a vegetation community comparable to natural freshwater tidal marshes was observed in the studied restored marsh (Jacobs et al., 2009; Oosterlee et al., 2017). This might be due to the relatively high net accretion rate of around 0.04 m yr^{-1} in the intermediate elevated parts of the marsh (Vandenbruwaene et al., 2011).

4.4. Implications for marsh restoration and management

Soil compaction affects subsurface hydrology in restored tidal wetlands and is therefore a widespread problem in restoration projects. To enhance surface drainage and to jumpstart further creek formation, in some marsh restoration projects, artificial creek networks are excavated in formerly embanked agricultural land before marsh restoration (e.g. Eertman et al., 2002). We expect that such creek initiation would also enhance groundwater seepage, but, according to our results, only within the first few meters from the creek edges. To increase infiltration and drainage in the marsh interior, we argue that methods should be sought to increase the hydraulic conductivity of compacted relict soil layers. One of these methods could be deep ploughing, as proposed by Brooks et al. (2015) or amending the soil with organic wastes to induce the development of macropore networks. Further research should indicate whether implementation of these methods would effectively enhance groundwater flow and biogeochemical cycling in restored tidal marshes.

5. Conclusions

When tidal marshes are restored on formerly embanked agricultural land that has been subjected to soil compaction, groundwater level fluctuations are restricted to the layer of newly deposited sediment. This layer has a high hydraulic conductivity, organic matter content, macroporosity and a low bulk density. However, the underlying layer of relict agricultural polder soil, which has a very low hydraulic conductivity, a low micro- and macroporosity, a low organic matter content and a high bulk density, forms an impermeable layer for groundwater. As a result, drainage in restored tidal marshes is hindered, which supposedly affects both vegetation development and nutrient cycling. Both the hydraulic conductivity (which was found to be affected by the macroporosity), and the distance from a creek are determining groundwater level fluctuations in tidal marshes. Therefore, both these factors should be considered in restoration schemes.

Acknowledgements

We would like to thank Dimitri Van Pelt and Simon De Meulenaer for field assistance. We are grateful to MeteoMoes for providing barometric data. Niels Van Putte and Marjolein Heyndrickx are SB PhD Fellow at FWO (project no. 1S17517N and 1S02016N, respectively). The Ghent University Special Research (BOF-UGent) is acknowledged for the financial support to the Centre of Expertise UGCT (BOF.EXP.2017.000007). The authors have no conflict of interest to declare.

Appendix A. Supplementary data

Supplementary data related to this article can be found at https://doi.org/10.1016/j.ecss.2019.02.006.

References

Bakker, J.P., Esselink, P., Dijkema, K.S., van Duin, W.E., de Jong, D.J., 2002. Restoration of salt marshes in The Netherlands. Hydrobiologia 478, 29–51. https://doi.org/10.1023/A:1021066311728.

Ballantine, K.A., Lehmann, J., Schneider, R.L., Groffman, P.M., 2015. Trade-offs between soil-based functions in wetlands restored with soil amendments of differing lability. Ecol. Appl. 25, 215–225. https://doi.org/10.1890/13-1409.1.

Bantilan-Smith, M., Bruland, G.L., MacKenzie, R.A., Henry, A.R., Ryder, C.R., 2009. A comparison of the vegetation and soils of natural, restored, and created coastal lowland wetlands in Hawaii. Wetlands 29, 1023–1035. https://doi.org/10.1672/08-127.1.

Barbier, E.B., Hacker, S.D., Kennedy, C., Koch, E.W., Stier, A.C., Silliman, B.R., 2011. The value of estuarine and coastal ecosystem services. Ecol. Monogr. 81, 169–193. https://doi.org/10.1890/10-1510.1.

Barrett, J.F., Keat, N., 2004. Artifacts in CT: recognition and avoidance. Radiographics 24, 1679–1691. https://doi.org/10.1148/rg.246045065.

Beauchard, O., Jacobs, S., Cox, T.J.S., Maris, T., Vrebos, D., Van Braeckel, A., Meire, P., 2011. A new technique for tidal habitat restoration: evaluation of its hydrological potentials. Ecol. Eng. 37, 1849–1858. https://doi.org/10.1016/j.ecoleng.2011.06.010.

Beauchard, O., Jacobs, S., Ysebaert, T., Meire, P., 2013. Sediment macroinvertebrate community functioning in impacted and newly-created tidal freshwater habitats. Estuar. Coast Shelf Sci. 120, 21–32. https://doi.org/10.1016/j.ecss.2013.01.013.
Beven, K., Germann, P., 1982. Macropores and water-flow in soils. Water Resour. Res. 18, 1311–1325. https://doi.org/10.1029/WR018i005p01311.
Beven, K., Germann, P., 2013. Macropores and water flow in soils revisited. Water Resour. Res. 49, 3071–3092. https://doi.org/10.1002/wrcr.20156.
Blackwell, M.S.A., Hogan, D.V., Maltby, E., 2004. The short-term impact of managed realignment on soil environmental variables and hydrology. Estuar. Coast Shelf Sci. 59, 687–701. https://doi.org/10.1016/j.ecss.2003.11.012.
Boorman, L.A., Hazelden, J., 2017. Managed re-alignment; a salt marsh dilemma? Wetl. Ecol. Manag. 1–17. https://doi.org/10.1007/s11273-017-9556-9.
Brabant, L., Vlassenbroeck, J., De Witte, Y., Cnudde, V., Boone, M.N., Dewanckele, J., Van Hoorebeke, L., 2011. Three-dimensional analysis of high-resolution X-ray computed tomography data with Morpho+. Microsc. Microanal. 17, 252–263. https://doi.org/10.1017/S1431927610094389.
Brooks, K.L., Mossman, H.L., Chitty, J.L., Grant, A., 2015. Limited vegetation development on a created salt marsh associated with over-consolidated sediments and lack of topographic heterogeneity. Estuar. Coast. 38, 325–336. https://doi.org/10.1007/s12237-014-9824-3.
Byers, S.E., Chmura, G.L., 2014. Observations on shallow subsurface hydrology at bay of fundy macrotidal salt marshes. J. Coast Res. 30, 1006–1016. https://doi.org/10.2112/Jcoastres-D-12-00167.1.
Cao, M., Xin, P., Jin, G.Q., Li, L., 2012. A field study on groundwater dynamics in a salt marsh - chongming Dongtan wetland. Ecol. Eng. 40, 61–69. https://doi.org/10.1016/j.ecoleng.2011.12.018.
Chapman, V.J., 1938. Studies in salt-marsh ecology sections I to III. J. Ecol. 26, 144–179. https://doi.org/10.2307/2256416.
Cnudde, V., Boone, M.N., 2013. High-resolution X-ray computed tomography in geosciences: a review of the current technology and applications. Earth Sci. Rev. 123, 1–17. https://doi.org/10.1016/j.earscirev.2013.04.003.
Costanza, R., dArge, R., deGroot, R., Farber, S., Grasso, M., Hannon, B., Limburg, K., Naeem, S., ONeill, R.V., Paruelo, J., Raskin, R.G., Sutton, P., vandenBelt, M., 1997. The value of the world's ecosystem services and natural capital. Nature 387, 253–260. https://doi.org/10.1038/387253a0.
Cox, T.J.S., 2017. Tides R-Package v2.0: Muddy One. https://doi.org/10.5281/zenodo.897843.
Cox, T.J.S., Maris, T., De Vleeschauwer, P., De Mulder, T., Soetaert, K., Meire, P., 2006. Flood control areas as an opportunity to restore estuarine habitat. Ecol. Eng. 28, 55–63. https://doi.org/10.1016/j.ecoleng.2006.04.001.
Craft, C.B., Seneca, E.D., Broome, S.W., 1991. Porewater chemistry of natural and created marsh soils. J. Exp. Mar. Biol. Ecol. 152, 187–200. https://doi.org/10.1016/0022-0981(91)90214-H.
Crooks, S., Pye, K., 2000. Sedimentological controls on the erosion and morphology of saltmarshes: implications for flood defence and habitat recreation. Geol. Soc. Spec. Publ. 175, 207–222. https://doi.org/10.1144/Gsl.Sp.2000.175.01.16.
Di Bella, C.E., Rodriguez, A.M., Jacobo, E., Golluscio, R.A., Taboada, M.A., 2015. Impact of cattle grazing on temperate coastal salt marsh soils. Soil Use Manag. 31, 299–307. https://doi.org/10.1111/sum.12176.
Dijkema, K.S., 1987. Changes in salt-marsh area in The Netherlands wadden sea after 1600. In: Huiskes, A.H.L., Blom, C.W.P.M., Rozema, J. (Eds.), Vegetation between Land and Sea: Structure and Processes. Springer Netherlands, Dordrecht, pp. 42–51.
Drabsch, J.M., Parnell, K.E., Hume, T.M., Dolphin, T.J., 1999. The capillary fringe and the water table in an intertidal estuarine sand flat. Estuar. Coast Shelf Sci. 48, 215–222. https://doi.org/10.1006/ecss.1998.0414.
Eertman, R.H.M., Kornman, B.A., Stikvoort, E., Verbeek, H., 2002. Restoration of the Sieperda tidal marsh in the Scheldt estuary, The Netherlands. Restor. Ecol. 10, 438–449. https://doi.org/10.1046/j.1526-100X.2002.01034.x.
Eijkelkamp Agrisearch Equipments, 2013. Laboratory-Permeameters: Operation Instructions. Giesbeek, The Netherlands.
Elschot, K., Bouma, T.J., Temmerman, S., Bakker, J.P., 2013. Effects of long-term grazing on sediment deposition and salt-marsh accretion rates. Estuar. Coast Shelf Sci. 133, 109–115. https://doi.org/10.1016/j.ecss.2013.08.021.
European Parliament and the Council of the European Union, 2000. Directive 2000/60/EC of the European Parliament and of the Council establishing a framework for the Community action in the field of water policy. Off. J. Eur. Commun. L327 22.12.2000.
French, P.W., 2006. Managed realignment - the developing story of a comparatively new approach to soft engineering. Estuar. Coast Shelf Sci. 67, 409–423. https://doi.org/10.1016/j.ecss.2005.11.035.
Garbutt, A., Wolters, M., 2008. The natural regeneration of salt marsh on formerly reclaimed land. Appl. Veg. Sci. 11, 335–344. https://doi.org/10.3170/2008-7-18451.
Garbutt, R.A., Reading, C.J., Wolters, M., Gray, A.J., Rothery, P., 2006. Monitoring the development of intertidal habitats on former agricultural land after the managed realignment of coastal defences at Tollesbury, Essex, UK. Mar. Pollut. Bull. 53, 155–164. https://doi.org/10.1016/j.marpolbul.2005.09.015.
Gardner, L.R., 2005. Role of geomorphic and hydraulic parameters in governing pore water seepage from salt marsh sediments. Water Resour. Res. 41. https://doi.org/10.1029/2004wr003671.
Gedan, K.B., Kirwan, M.L., Wolanski, E., Barbier, E.B., Silliman, B.R., 2011. The present and future role of coastal wetland vegetation in protecting shorelines: answering recent challenges to the paradigm. Clim. Change 106, 7–29. https://doi.org/10.1007/s10584-010-0003-7.
Harvey, J.W., Chambers, R.M., Hoelscher, J.R., 1995. Preferential flow and segregation of porewater solutes in wetland sediment. Estuaries 18, 568–578. https://doi.org/10.2307/1352377.
Harvey, J.W., Germann, P.F., Odum, W.E., 1987. Geomorphological control of subsurface hydrology in the creek-bank zone of tidal marshes. Estuar. Coast Shelf Sci. 25, 677–691. https://doi.org/10.1016/0272-7714(87)90015-1.
Hazelden, J., Boorman, L.A., 2001. Soils and 'managed retreat' in south east England. Soil Use Manag. 17, 150–154. https://doi.org/10.1079/Sum200166.
Heinsch, F.A., Heilman, J.L., McInnes, K.J., Cobos, D.R., Zuberer, D.A., Roelke, D.L., 2004. Carbon dioxide exchange in a high marsh on the Texas Gulf Coast: effects of freshwater availability. Agric. For. Meteorol. 125, 159–172. https://doi.org/10.1016/j.agrformat.2004.02.007.
Heiri, O., Lotter, A.F., Lemcke, G., 2001. Loss on ignition as a method for estimating organic and carbonate content in sediments: reproducibility and comparability of results. J. Paleolimnol. 25, 101–110. https://doi.org/10.1023/a:1008119611481.
Hemond, H.F., Fifield, J.L., 1982. Subsurface flow in salt-marsh peat - a model and field-study. Limnol. Oceanogr. 27, 126–136. https://doi.org/10.4319/lo.1982.27.1.0126.
Howes, B.L., Howarth, R.W., Teal, J.M., Valiela, I., 1981. Oxidation-reduction potentials in a salt-marsh - spatial patterns and interactions with primary production. Limnol. Oceanogr. 26, 350–360. https://doi.org/10.4319/lo.1981.26.2.0350.
Hughes, C.E., Binning, P., Willgoose, G.R., 1998. Characterisation of the hydrology of an estuarine wetland. J. Hydrol. 211, 34–49. https://doi.org/10.1016/S0022-1694(98)00194-2.
Iost, S., Landgraf, D., Makeschin, F., 2007. Chemical soil properties of reclaimed marsh soil from Zhejiang Province PR China. Geoderma 142, 245–250. https://doi.org/10.1016/j.geoderma.2007.08.001.
Jacobs, S., Beauchard, O., Struyf, E., Cox, T.J.S., Maris, T., Meire, P., 2009. Restoration of tidal freshwater vegetation using controlled reduced tide (CRT) along the Schelde Estuary (Belgium). Estuar. Coast Shelf Sci. 85, 368–376. https://doi.org/10.1016/j.ecss.2009.09.004.
Jacobs, S., Struyf, E., Maris, T., Meire, P., 2008. Spatiotemporal aspects of silica buffering in restored tidal marshes. Estuar. Coast Shelf Sci. 80, 42–52. https://doi.org/10.1016/j.ecss.2008.07.003.
Kadiri, M., Spencer, K.L., Heppell, C.M., Fletcher, P., 2011. Sediment characteristics of a restored saltmarsh and mudflat in a managed realignment scheme in Southeast England. Hydrobiologia 672, 79–89. https://doi.org/10.1007/s10750-011-0755-8.
Kolditz, K., Dellwig, O., Barkowski, J., Beck, M., Freund, H., Brumsack, H.J., 2009. Effects of de-embankment on pore water geochemistry of salt marsh sediments. J. Coast Res. 25, 1222–1235. https://doi.org/10.2112/08-1053.1.
Kong, J., Xin, P., Hua, G.F., Luo, Z.Y., Shen, C.J., Chen, D., Li, L., 2015. Effects of vadose zone on groundwater table fluctuations in unconfined aquifers. J. Hydrol. 528, 397–407. https://doi.org/10.1016/j.jhydrol.2015.06.045.
Luo, L.F., Lin, H., Li, S.C., 2010. Quantification of 3-D soil macropore networks in different soil types and land uses using computed tomography. J. Hydrol. 393, 53–64. https://doi.org/10.1016/j.jhydrol.2010.03.031.
Ma, Z., Melville, D.S., Liu, J., Chen, Y., Yang, H., Ren, W., Zhang, Z., Piersma, T., Li, B., 2014. Rethinking China's new great wall: massive seawall construction in coastal wetlands threatens biodiversity. Science 346, 912–914. https://doi.org/10.1126/science.1257258.
Maris, T., Cox, T.J.S., Temmerman, S., De Vleeschauwer, P., Van Damme, S., De Mulder, T., Van den Bergh, E., Meire, P., 2007. Tuning the tide: creating ecological conditions for tidal marsh development in a flood control area. Hydrobiologia 588, 31–43. https://doi.org/10.1007/s10750-007-0650-5.
Masschaele, B., Dierick, M., Van Loo, D., Boone, M.N., Brabant, L., Pauwels, E., Cnudde, V., Van Hoorebeke, L., 2013. HECTOR: a 240kV micro-CT setup optimized for research. J. Phys. Conf. 463, 012012. https://doi.org/10.1088/1742-6596/463/1/012012.
Mcleod, E., Chmura, G.L., Bouillon, S., Salm, R., Bjork, M., Duarte, C.M., Lovelock, C.E., Schlesinger, W.H., Silliman, B.R., 2011. A blueprint for blue carbon: toward an improved understanding of the role of vegetated coastal habitats in sequestering CO2. Front. Ecol. Environ. 9, 552–560. https://doi.org/10.1890/110004.
Meire, P., Ysebaert, T., Van Damme, S., Van den Bergh, E., Maris, T., Struyf, E., 2005. The Scheldt estuary: a description of a changing ecosystem. Hydrobiologia 540, 1–11. https://doi.org/10.1007/s10750-005-0896-8.
Mendelssohn, I.A., Seneca, E.D., 1980. The influence of soil drainage on the growth of salt-marsh cordgrass spartina-alterniflora in north-carolina. Estuar. Coast Mar. Sci. 11, 27–40. https://doi.org/10.1016/S0302-3524(80)80027-2.
Moffett, K.B., Gorelick, S.M., McLaren, R.G., Sudicky, E.A., 2012. Salt marsh ecohydrological zonation due to heterogeneous vegetation–groundwater–surface water interactions. Water Resour. Res. 48. https://doi.org/10.1029/2011WR010874.
Montalto, F.A., Parlange, J.Y., Steenhuis, T.S., 2007. A simple model for predicting water table fluctuations in a tidal marsh. Water Resour. Res. 43. https://doi.org/10.1029/2004wr003913.
Montalto, F.A., Steenhuis, T.S., 2004. The link between hydrology and restoration of tidal marshes in the New York New Jersey Estuary. Wetlands 24, 414–425. https://doi.org/10.1672/0277-5212(2004)024[0414:Tlbhar]2.0.Co;2.
Montalto, F.A., Steenhuis, T.S., Parlange, J.Y., 2006. The hydrology of Piermont Marsh, a reference for tidal marsh restoration in the Hudson river estuary, New York. J. Hydrol. 316, 108–128. https://doi.org/10.1016/j.jhydrol.2005.03.043.
Mossman, H.L., Davy, A.J., Grant, A., 2012. Does managed coastal realignment create saltmarshes with 'equivalent biological characteristics' to natural reference sites? J. Appl. Ecol. 49, 1446–1456. https://doi.org/10.1111/j.1365-2664.2012.02198.x.
Nolte, S., Muller, F., Schuerch, M., Wanner, A., Esselink, P., Bakker, J.P., Jensen, K., 2013. Does livestock grazing affect sediment deposition and accretion rates in salt marshes? Estuar. Coast Shelf Sci. 135, 296–305. https://doi.org/10.1016/j.ecss.2013.10.026.
Nuttle, W.K., 1988. The extent of lateral water-movement in the sediments of a new England salt-marsh. Water Resour. Res. 24, 2077–2085. https://doi.org/10.1029/WR024i012p02077.
O'Connor, M.T., Moffett, K.B., 2015. Groundwater dynamics and surface water-

groundwater interactions in a prograding delta island, Louisiana, USA. J. Hydrol. 524, 15–29. https://doi.org/10.1016/j.jhydrol.2015.02.017.
Oosterlee, L., Cox, T.J.S., Vandenbruwaene, W., Maris, T., Temmerman, S., Meire, P., 2017. Tidal marsh restoration design affects feedbacks between inundation and elevation change. Estuar. Coast. https://doi.org/10.1007/s12237-017-0314-2.
Portnoy, J.W., 1999. Salt marsh diking and restoration: biogeochemical implications of altered wetland hydrology. Environ. Manag. 24, 111–120. https://doi.org/10.1007/s002679900219.
R Development Core Team, 2015. R: A Language and Environment for Statistical Computing. R Foundation for Statistical Computing, Vienna, Austria.
Schmitz, A., Harrison, J.F., 2004. Hypoxic tolerance in air-breathing invertebrates. Respir. Physiol. Neurobiol. 141, 229–242. https://doi.org/10.1016/j.resp.2003.12.004.
Sloey, T.M., Hester, M.W., 2016. Interactions between soil physicochemistry and belowground biomass production in a freshwater tidal marsh. Plant Soil 401, 397–408. https://doi.org/10.1007/s11104-015-2760-6.
Soille, P., 1999. Morphological Image Analysis. Springer-Verlag, Berlin, Heidelberg, New York.
Spencer, K.L., Carr, S.J., Diggens, L.M., Tempest, J.A., Morris, M.A., Harvey, G.L., 2017. The impact of pre-restoration land-use and disturbance on sediment structure, hydrology and the sediment geochemical environment in restored saltmarshes. Sci. Total Environ. 587, 47–58. https://doi.org/10.1016/j.scitotenv.2016.11.032.
Spencer, K.L., Cundy, A.B., Davies-Hearn, S., Hughes, R., Turner, S., MacLeod, C.L., 2008. Physicochemical changes in sediments at Orplands Farm, Essex, UK following 8 years of managed realignment. Estuar. Coast Shelf Sci. 76, 608–619. https://doi.org/10.1016/j.ecss.2007.07.029.
Struyf, E., Temmerman, S., Meire, P., 2007. Dynamics of biogenic Si in freshwater tidal marshes: Si regeneration and retention in marsh sediments (Scheldt estuary). Biogeochemistry 82, 41–53. https://doi.org/10.1007/s10533-006-9051-5.
Susilo, A., Ridd, P.V., 2005. The bulk hydraulic conductivity of mangrove soil perforated with animal burrows. Wetl. Ecol. Manag. 13, 123–133. https://doi.org/10.1007/s11273-004-8324-9.
Tempest, J.A., Harvey, G.L., Spencer, K.L., 2015. Modified sediments and subsurface hydrology in natural and recreated salt marshes and implications for delivery of ecosystem services. Hydrol. Process. 29, 2346–2357. https://doi.org/10.1002/hyp.10368.
Udden, J.A., 1914. Mechanical composition of clastic sediments. Geol. Soc. Am. Bull. 25, 655–744. https://doi.org/10.1130/GSAB-25-655.
Ursino, N., Silvestri, S., Marani, M., 2004. Subsurface flow and vegetation patterns in tidal environments. Water Resour. Res. 40. https://doi.org/10.1029/2003wr002702.
Vandenbruwaene, W., Maris, T., Cox, T.J.S., Cahoon, D.R., Meire, P., Temmerman, S., 2011. Sedimentation and response to sea-level rise of a restored marsh with reduced tidal exchange: comparison with a natural tidal marsh. Geomorphology 130, 115–126. https://doi.org/10.1016/j.geomorph.2011.03.004.
Vandenbruwaene, W., Meire, P., Temmerman, S., 2012. Formation and evolution of a tidal channel network within a constructed tidal marsh. Geomorphology 151, 114–125. https://doi.org/10.1016/j.geomorph.2012.01.022.
Vlassenbroeck, J., Dierick, M., Masschaele, B., Cnudde, V., Hoorebeke, L., Jacobs, P., 2007. Software tools for quantification of X-ray microtomography. Nucl. Instrum. Methods A 580, 442–445. https://doi.org/10.1016/j.nima.2007.05.073.
Waterinfo, 2016. Neerslag, droogte, getijden en overstromingen, Vlaamse Milieumaatschappij, Waterbouwkundig Laboratorium, Maritieme Dienstverlening & Kust. Waterwegen en Zeekanaal NV & De Scheepvaart NV.
Wentworth, C.K., 1922. A scale of grade and class terms for clastic sediments. J. Geol. 30, 377–392. https://doi.org/10.1086/622910.
Wilson, A.M., Evans, T., Moore, W., Schutte, C.A., Joye, S.B., Hughes, A.H., Anderson, J.L., 2015. Groundwater controls ecological zonation of salt marsh macrophytes. Ecology 96, 840–849. https://doi.org/10.1890/13-2183.1.
Wilson, A.M., Gardner, L.R., 2006. Tidally driven groundwater flow and solute exchange in a marsh: numerical simulations. Water Resour. Res. 42. https://doi.org/10.1029/2005wr004302.
Wolters, M., Garbutt, A., Bakker, J.P., 2005. Salt-marsh restoration: evaluating the success of de-embankments in north-west Europe. Biol. Conserv. 123, 249–268. https://doi.org/10.1016/j.biocon.2004.11.013.
Xia, Y.Q., Li, H.L., 2012. A combined field and modeling study of groundwater flow in a tidal marsh. Hydrol. Earth Syst. Sci. 16, 741–759. https://doi.org/10.5194/hess-16-741-2012.
Xin, P., Gibbes, B., Li, L., Song, Z.Y., Lockington, D., 2010. Soil saturation index of salt marshes subjected to spring-neap tides: a new variable for describing marsh soil aeration condition. Hydrol. Process. 24, 2564–2577. https://doi.org/10.1002/hyp.7670.
Xin, P., Jin, G.Q., Li, L., Barry, D.A., 2009. Effects of crab burrows on pore water flows in salt marshes. Adv. Water Resour. 32, 439–449. https://doi.org/10.1016/j.advwatres.2008.12.008.
Xin, P., Kong, J., Li, L., Barry, D.A., 2013. Modelling of groundwater-vegetation interactions in a tidal marsh. Adv. Water Resour. 57, 52–68. https://doi.org/10.1016/j.advwatres.2013.04.005.
Xin, P., Yu, X.Y., Lu, C.H., Li, L., 2016. Effects of macro-pores on water flow in coastal subsurface drainage systems. Adv. Water Resour. 87, 56–67. https://doi.org/10.1016/j.advwatres.2015.11.007.
Xin, P., Yuan, L.R., Li, L., Barry, D.A., 2011. Tidally driven multiscale pore water flow in a creek-marsh system. Water Resour. Res. 47. https://doi.org/10.1029/2010wr010110.
Xin, P., Zhou, T.Z., Lu, C.H., Shen, C.J., Zhang, C.M., D'Alpaos, A., Li, L., 2017. Combined effects of tides, evaporation and rainfall on the soil conditions in an intertidal creek-marsh system. Adv. Water Resour. 103, 1–15. https://doi.org/10.1016/j.advwatres.2017.02.014.
Yelverton, G.F., Hackney, C.T., 1986. Flux of dissolved organic-carbon and pore water through the substrate of a *Spartina alterniflora* marsh in north-carolina. Estuar. Coast Shelf Sci. 22, 255–267. https://doi.org/10.1016/0272-7714(86)90116-2.